Journal of South American Earth Sciences 32 (2011) 49–57

Contents lists available at ScienceDirect

Journal of South American Earth Sciences

journal homepage: www.elsevier.com/locate/jsames

Magnetotellurics applied to the study of the Guaraní aquifer in Entre Ríos Province, N–E Argentina

Alicia Favetto*, Ana Curcio, Cristina Pomposiello

INGEIS–CONICET, Ciudad Universitaria, Pabellón INGEIS, Buenos Aires 1428, Argentina

ARTICLE INFO

Article history:
Received 22 December 2009
Accepted 5 March 2011

Keywords:
Guaraní Aquifer
Magnetotellurics
Chaco Paranense Basin

ABSTRACT

The South American Guaraní Aquifer System covers the entire Parana basin and part of the Chaco-Parana basin. This system is one of the most important groundwater reservoirs; it is shared by four neighboring countries covering an area larger than one million square kilometers.

The geological units closely related to the Guaraní Aquifer are the Piramboia and Botucatu Formations that consist of Triassic–Jurassic aeolian, fluvial and lacustrine sandstones, and the Serra Geral basalts with clastic intercalations. Serra Geral, an effusive Cretaceous complex, covers the sandstones and provides a high degree of confinement to the system.

This paper presents the interpretation of magnetotelluric (MT) data collected during 2007–2008 in Entre Ríos Province, Argentina. These data, recorded in three profiles, mainly provide the depth to the crystalline basement, determinant for the presence of aquifer-related sediments. Models showed that the discrimination of the basalts strongly depends on local electrical characteristics. Model information is quite consistent with the information from oil and thermal wells located close to the profiles.

1. Introduction

The main characteristics of the Guaraní Aquifer System (Sistema Acuifero Guaraní, SAG) have been described by many scientists from different disciplines and institutions in the four countries that share the Guaraní Aquifer System (Brazil, Argentina, Paraguay and Uruguay). Attempts have been made to find a unique model for the aquifer, but the existing information is still not enough, mostly because of the large area of the SAG (see Fig. 1).

Very different geological, hydrogeological, hydraulic, hydrochemical and thermal characteristics of SAG are different in both Parana and Chaco-Parana basins (see e.g. Campos, 2000). Moreover, they are controlled by variations in the depositional environment; the structural evolution and the residence time of water within the formations, giving rise to heterogeneities and showing the presence of compartments.

Aquifer water is within Permian-Cretaceous sandstones, underlying Jurassic–Cretaceous basalts of varying degree of fracturing and fissuring. The most important recharge source of this confined aquifer is infiltrating rainfall where basalt is not present (e.g. Montaño et al., 2004). Groundwater flows from NE to SW and the temperature gradient follows the flow direction (from 22 ° to 60 °C), which is attributed mostly to the normal geothermal gradient (e.g. Tujchneider et al., 2006; Araújo et al., 1999).

The system thickness ranges from zero to around 800 m. Contours obtained from oil and deep-water wells show average estimates of the aquifer top and basalt thickness (Fig. 2). These values often seem to be strongly correlated with basement top irregularities. Subsurface electrical resistivity is known to contribute to a better understanding of complex aquifer systems by mapping the main geometry of the controlling structures. Resistivity distribution is useful to identify regions of increased permeability and fluid content, as well as conductive alteration due to induced fracturing. In Entre Ríos, geoelectrical studies were performed mostly during the last decade and deep wells were drilled to explore thermal resources.

The magnetotelluric method (MT) is suitable to map electrical resistivity as proven by numerous applications to geothermal exploration (see e.g. Arango et al., 2009; Bernard et al., 1998; Volpia et al., 2003). MT can provide an excellent image of subsurface formations down to depths of 1–10 km and depending on the magnetometer features, the prospected depth can be increased to hundreds of kilometers. Considering the deep structures that need to be studied for the characterization of the SAG, MT studies may improve the results of standard exploring methods like VES (Vertical Electric Sounding) (Favetto et al., 2005).

From 2004 to 2006 one W-E MT profile crossing the provinces of Santa Fé and Entre Rios at 31.5°S was performed using long period

* Corresponding author. Tel.: +54 1147833022; fax: +54 1147833024.
E-mail address: favetto@ingeis.uba.ar (A. Favetto).

0895-9811/$ – see front matter © 2011 Elsevier Ltd. All rights reserved.
doi:10.1016/j.jsames.2011.03.005

Fig. 1. Map showing the extent of the SAG in South America, the boundaries between the countries sharing the SAG (Brazil, Argentina, Paraguay and Uruguay) and the estimated aquifer boundary. The study area is also indicated.

Flux Gate magnetometers. This was our first MT survey in the SAG area (Favetto and Pomposiello, 2009).

The profile belongs to a large-scale research project on the crust and mantle related to the Pampean Ranges and the Chaco Pampean Plain (e.g. Booker et al., 2004; Favetto et al., 2008).

This study focuses on determining the basin geometry in an area believed to include the SAG. In some areas, our resistivity models permit differentiating basalt from over and underlying sediments, but in others with very low sediment resistivity, saline fluids penetrate into fractures in the basalt and make the basalt very conductive and thus it is difficult to discriminate, from the geoelectrical model, the basalts from the sediments. However, the interface between sediments (which may include basalts) and the resistive basement is clearly resolved everywhere. There is good agreement between our models and the lithologic interpretation in wells drilled for thermal exploration.

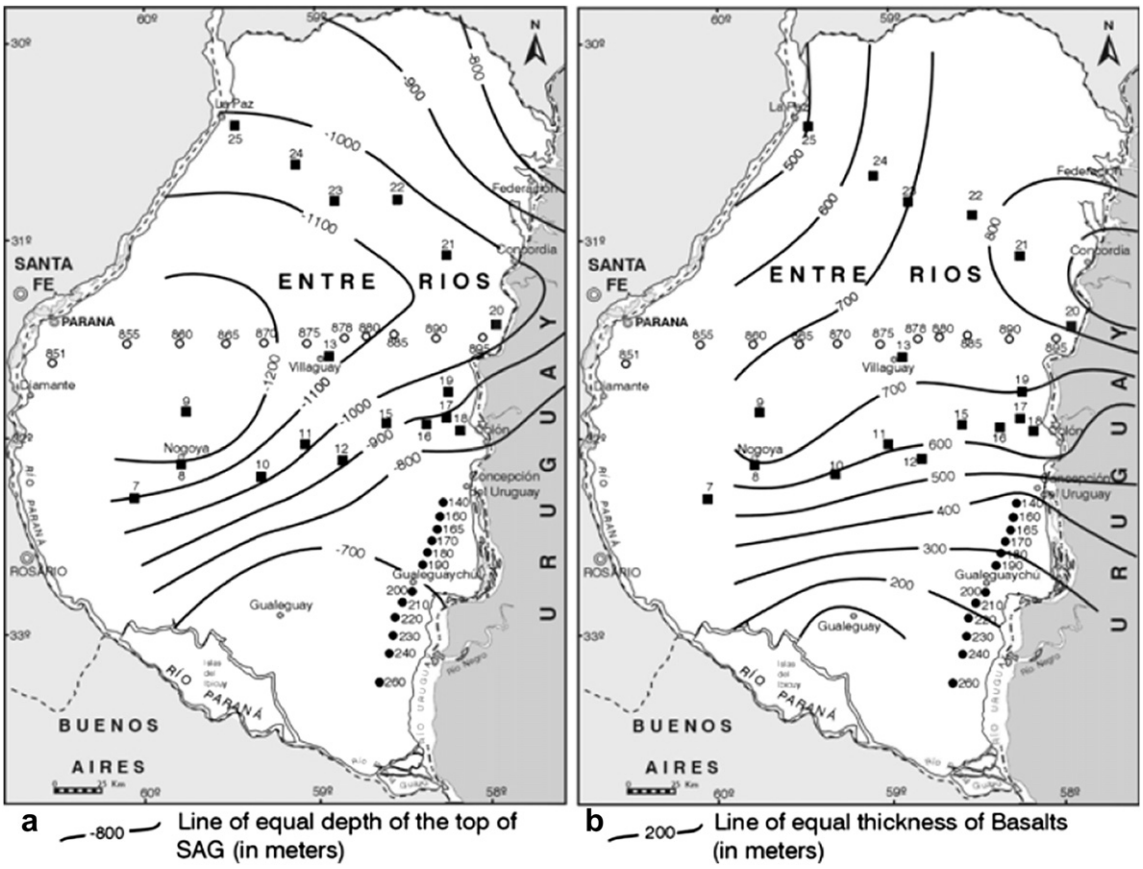

Fig. 2. Contours in Entre Ríos Province inferred from deep wells. a) SAG top depth contours in meters. b) Thickness contours for Serra Geral Formation (Modified from Silva Busso, 1999, p. 252).

2. Study area

The hydrogeological features of the system vary significantly across the Paraná and Chaco- Paraná basins. These variations are mainly attributed to the structural depositional environments of the basins, flow records and water residence time (Araújo et al., 1999). The part of the SAG in the Chaco- Paraná basin is smaller and its western and southern boundaries remain unknown. It covers an area of about 350,000 km^2 in the Chaco- Paraná basin, from which about 225,000 km^2 are located in northeastern Argentina.

In Entre Ríos, the aquifer system is formed by two subsystems: one, in the north-centere of the province, with low salinity water and higher temperatures and the other, near the southern border of the aquifer system in Argentina, with high salinity and lower temperatures (Montaño et al., 1998). The southern border of the aquifer has not been defined yet, even though existing evidence suggests that it is placed in the south of Entre Rios Province.

3. Geologic and hydrogeologic framework

The Chaco pampean plain is part of the Central Andean distal piedmont which was generated from the uplifting and erosion of the Andean Cordillera as a result of the subduction of the Nazca plate beneath the South American plate (see e.g. Ramos et al., 2002). The plain has not been significant deformation by tectonic processes occurred since the Tertiary and a continuous layer of Quaternary loess has covered it. Beneath the plain, strong variations in the thickness of the sedimentary column indicate the presence of depocenters of different ages and geological settings (see e.g. Chebli et al., 1999). In particular, the Chaco-Parana basin has received all the sediments coming from the uplifting of the Andes since the Miocene. The main SAG-related geological units are Triassic–Jurassic aeolian and fluvial sandstones of the Piramboia and Botucatu Formations (Sanford and Lange, 1960). The Serra Geral (White, 1908) Cretaceous basaltic formation provides different confining degree to the aquifer with possible presence of clastic intercalations (Solari Member; Gentili and Rimoldi, 1979). In Entre Ríos, the depth of the crystalline basement top is the main structural factor determining the presence of sediments containing the SAG. The crystalline basement is formed by the most ancient rocks in the region and consists predominantly of metamorphic and igneous rocks, exposed in the island of Martin Garcia and in Uruguay.

The integrated SAG-related stratigraphic column with a rough description of the lithological and hydrogeological features of the different units of the Entre Ríos Province is shown in Table 1 and relevant data from oil and thermal wells located in that area are shown in Table 2 (drilling depth, meters drilled into SAG, top and bottom depths of the basalts in meters and the depth to the basement when it was reached).

4. Magnetotelluric method

The MT method is an electromagnetic technique to measure variations in the natural electromagnetic fields. It is used to investigate the electrical resistivity structure of the subsurface, from depths of tens of meters to hundreds of kilometers. Under the plane wave assumption, the natural electromagnetic wave

Table 1
SAG-related integrated stratigraphic column, following Favetto et al., 2005 and therein cited documents.

Age	Unit	Lithology	Hydrogeologic behavior
Cretaceous	*Serra Geral* Formation. (*Serra Geral* and *Solari Member*)	Tholeititic basalts and clastic intercalations partially silicified	Basalts: aquifer (fractured rock) to aquifuge. Sandstones: aquifer
Jurassic	*Botucatu* Formation	Reddish fine sandstones partially local silicified	aquifer
Triassic	*Piramboia* Formation	Upper: fine to medium sandstones Lower: fine sandstones with clay lenses and claystones	aquifer
Lower Paleozoic to Precambrian	*Crystalline basement*	Igneous and metamorphic rocks aquifuge	aquifuge

propagates vertically into the Earth. The magnetic field and the electric field components are recorded at the Earth's surface. The penetration depth of these signals increases with period and resistivity (e.g. Bahr and Simpson, 2005). Using the Fourier-Transform, the time-series obtained were converted into frequencies, which were then used to derive the impedance tensor, Z. The linear relationship between the horizontal components of the magnetic (H_x, H_y) and electric (E_x, E_y) fields (with x to the north and y to the east) for each period (τ) or frequency, ($f = 1/\tau$) is expressed as:

$E_x = Z_{xx}H_x + Z_{xy}H_y$

$E_y = Z_{yx}H_x + Z_{yy}H_y$

The impedance tensor, a complex magnitude, was rotated into principal directions and then converted to apparent resistivity (ρ) and phase (φ), defined as:

$$\rho_{ij}(f) = \frac{1}{2\pi f \mu}|Z_{ij}(f)|^2$$

$$\varphi_{ij}(f) = \tan^{-1}\frac{\mathrm{Im}(Z_{ij}(f))}{\mathrm{Re}(Z_{ij}(f))}$$

where, μ is the magnetic permeability, and i, j denote horizontal components.

In the two dimension case (2D), in which the resistivity structure varies with depth and in only one horizontal direction, MT fields can be decomposed into transverse-electric (TE) and transverse-magnetic (TM) modes. Due to the depths involved, MT is a very convenient technique for imaging the resistivity distribution and characterizing the structures that control aquifer systems.

Table 2
Thermal and oil wells drilled in the province of Entre Ríos, basalt depth and thickness, basement top and meters drilled into the SAG (from Mársico, 2009).

Well name	Depth (m)	Meters in SAG	Geology		
			Basalts		Crystalline basement (m)
			From (m)	To (m)	
Diamante 1	1554	–	720	1554	nr > 1554
Victoria 1	1030	–	750	1050	nr > 1050
Gualeguaychú 1	1000	259	473	729	988
Gualeguaychú 2	825	180	450	635	815
Concepción del Uruguay	512	–	250	460	460
Basavilbaso	1258	195	523	1062	nr > 1257
Colón 1	1502	–	228	886	886
San José 1	885	63	282	802	nr > 865
Villa Elisa 1	1030	48	348	982	nr > 1030
Concordia 2	1142	127	54	1015	nr > 114
La Paz 1	1001	181	478	820	nr > 1001
Ma. Grande 1	1376	–	602	1376	nr > 1376
Villaguay-1	1357	63	444	1294	nr > 1354
Nogoyá	2088	648	662	1440	nr > 2088

nr: not reached.

4.1. Data acquisition and analysis

A total of 27 sites were acquired during 2007–08. Sites were distributed in three profiles of approximate N–S, W–E, and NW–SE directions. Profiles are called P-1, P-2 and P-3 respectively. Data in profile P-1 were collected with commercial wideband receivers (EMI MT-24) within a bandwidth of 0.01 to about 200 s and profiles P-2 and P-3 were collected with a Phoenix V8 system in the bandwidth from 0.002 to 100 s. The electric dipoles (with $PbCl_2$–KCl electrodes) and the magnetic sensor coils were aligned with geomagnetic coordinates.

The MT impedance tensor and the vertical to horizontal magnetic field transfer functions were estimated in the measurement coordinate system using the robust code (EMTF) of Egbert and Booker (1987).

The magnetotelluric profiles interpreted in this study and the location of the profile performed along a W–E transect at 31.5°S are shown in Fig. 3.

4.2. Dimensionality and distortions

The dimensionality and best geoelectrical strike estimation were studied using tensor decomposition (McNeice and Jones, 2001) and phase tensor analysis (Caldwell et al., 2004). Decomposing impedance tensors Z into real (X) and imaginary (Y) parts

$Z = X + i\,Y$

X and Y define the phase tensor ϕ as

$$\phi = X^{-1}Y$$

The phase tensor is graphically represented by an ellipse. An invariant parameter of this tensor is the skew angle defined as:

$$\text{Skew angle} = 1/2\tan^{-1}((\phi 12 - \phi 21)/(\phi 11 + \phi 22))$$

The phase tensor skew angle determines whether the 2D structure approximation is valid when its absolute value is less than 1.5° (Bibby et al., 2005). Another invariant, called ellipticity is defined as:

$$\lambda = ((\phi\max - \phi\min)/(\phi\max + \phi\min))$$

This parameter determines that the structure approximates to 1D when it takes values smaller than 0.1. This parameter was calculated at all the sites.

Fig. 4 shows the ellipticity, phase tensor skew angle and azimuth (orientation of the major axis which coincides with the strike in the 2D situation) at site 23, which can be considered representative of the average behavior of all sites. Skew angle is very small for periods shorter than 10 s and is smaller than 10° for most of the larger periods. Ellipticity is less than 0.1 for periods shorter than 1 s indicating a 1D structure for shallow depths. For periods longer

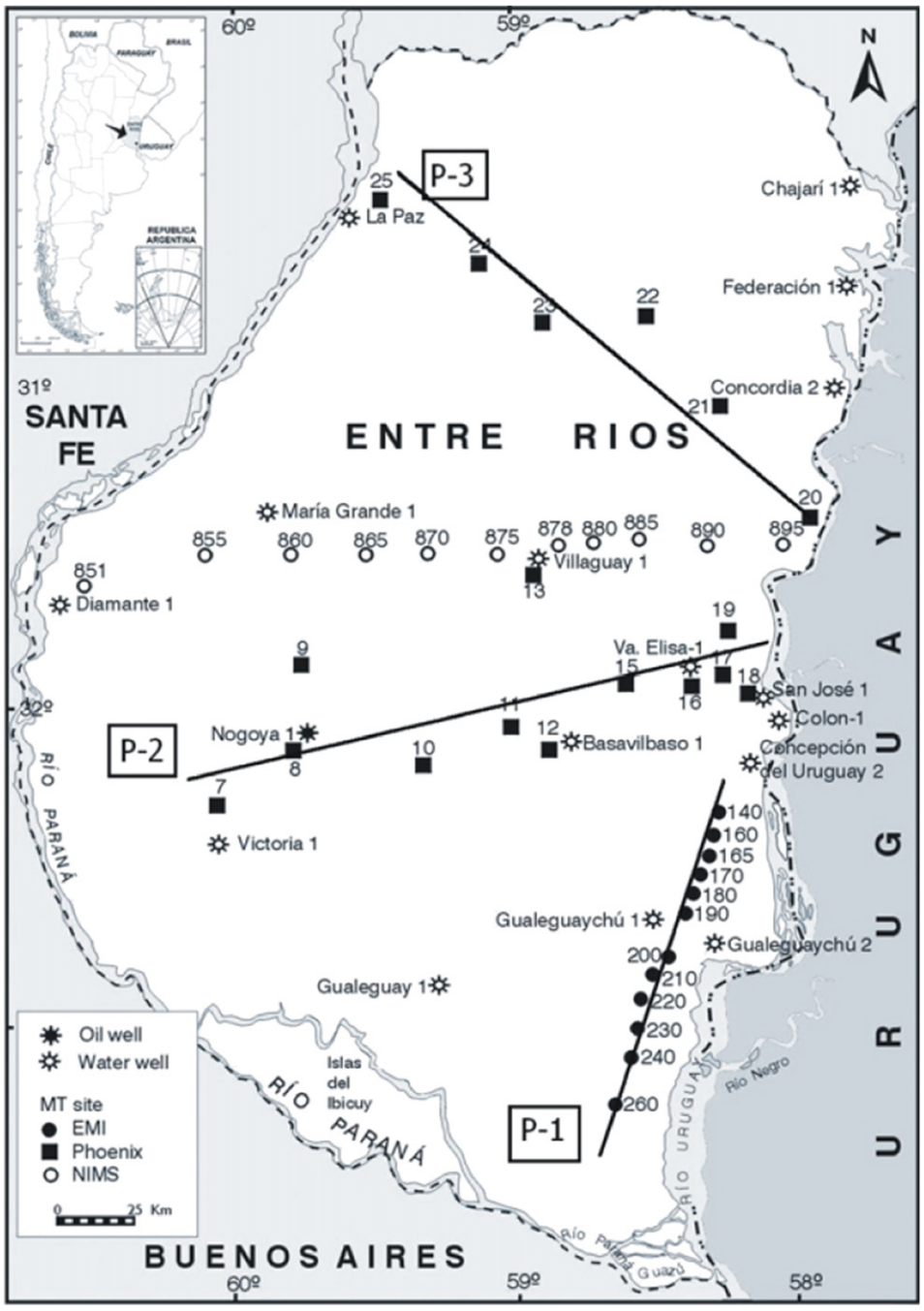

Fig. 3. Location of MT sites and wells in the province of Entre Ríos. Lines indicate MT profiles for P-1, P-2 and P-3.

than 1 s the structure can be considered as 2D. When the skew angle is close to zero, the azimuth calculated from the phase tensor coincides with one of the principal axes taking into account the 90° ambiguity to choose the strike direction. Strike values are more scattered for periods less than 1 s, as can expected in a 1D structure, and they are more stable from 1 to 100 s.

Multi-site and multi-frequency analyses were performed for each profile using the McNeice and Jones (2001) method on periods between 1 and 100 s, considering an error floor of 5% applied to the real and imaginary parts of the impedance tensor components. The processing of all the sites together for each profile gave strike values of 2.62 W°, 1.49 E° and 22.55 E° for profiles P-1, P-2 and P-3 respectively (with NRMS around 1).

This analysis also allows determining the shear and twist parameters. These parameters are descriptors of the degree of distortion of deeper structure by electric charges that form on very small-scale 3D features in the very shallow Earth.

In P-1 sites from 140 to 180, shear parameters lay in the range [−4°, 10°] and in sites from 204 to 260 those parameters are within [16°, 31°]. For all sites twist values are smaller than 13°. In P-2 and P-3, shear values are small and range from −10° to 10° at all sites. Exceptionally distorted are sites 7 and 25, placed at the end of profiles P-2 and P-3 where shear is larger. Twist values are small and within [−9°, 9°] except at sites 9, 11 and 18. The NRMS is low enough to consider that a 2D assumption is a good representation of the structure.

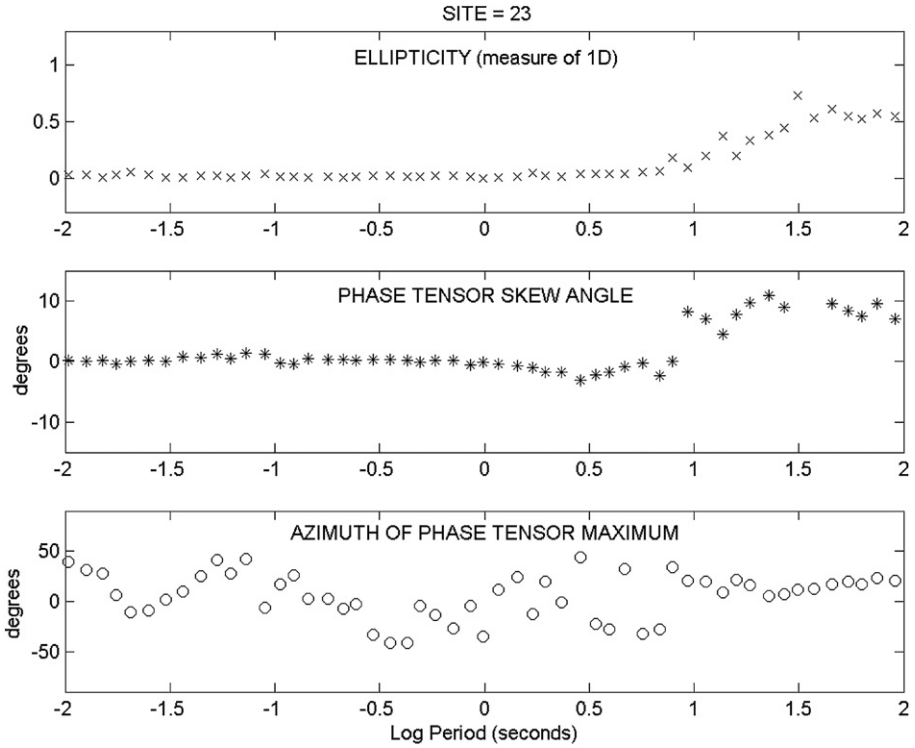

Fig. 4. Variation of dimensional parameters with period: ellipticity, skew and phase tensor azimuth for site 23, shown as an example.

4.3. 2D Modeling

Apparent resistivities (ρ_{TE} and ρ_{TM}) and impedance phases (φ_{TE} and φ_{TM}) decomposed into principal axes were used to obtain the models. P-1 strike direction was obtained rotating 90° due to geological evidences (see Fig. 2). At each site, phase data were tested for consistency with longer period data using the "rhoplus" algorithm of Parker and Booker (1996). T_{ZY} data were almost zero for short periods and very noisy for the last decade, so they have not been included in the inversion.

Both MT polarizations were jointly inverted using the NLCG algorithm of Rodi and Mackie (2001) included in the WinGLink interpretation software. Model roughness was minimized through an iterative algorithm up to a pre-established misfit. This was done by minimizing an objective function consisting of the χ^2 data misfit plus a trade-off parameter τ times the model roughness. In this paper roughness is defined as the integral of a Laplacian of the model, assuming a uniform Laplacian grid which means that the penalty on structure vertical roughness increases with depth at the same rate as the actual model block size.

The scale factor for roughness penalty β, is set to 1.0 and α is set to 0.5 for P-1 and 1 for P-2 and P-3. Selecting $\beta = 1$ means that the penalty on horizontal roughness increases with depth at the same rate as the vertical roughness. This means that the model will be smoother in both the vertical and horizontal directions as depth increases.

Furthermore, this code makes it possible to select tear areas within the model by turning off the smoothing across boundary function (e.g. Favetto et al., 2007). Many inversions were performed to achieve the most reliable model for each profile by testing both modes independently and adding tear discontinuities at the bottom of the basin. All the inversions started at 1000 Ohm-m half-space, since this value is more resistive than the highest resistivity found in the model. Static shift was corrected by fitting in the inversion processing after obtaining a good fitting of the data.

For profile P-1, evident differences were observed in the models of separate TE and TM inversions when including equal error floors. So, the TE apparent resistivity was completely removed from the inversion to avoid effects from off-profile sources. The P-1 model was obtained first, by inverting the TM mode. The basement-sediment discontinuity thus determined was included in a new inversion as tear constraint using TM (ρ_{TM} and φ_{TM}) and TE (φ_{TE}). Error floors were 10% for ρ_{TM}, 1.45° for φ_{TM} and 20% for φ_{TE}. The model for the P-1 profile and pseudosection measured data as well as model responses are shown in Fig. 5A.

Except for some details in profile P-2, the same model was achieved for TE and TM inversions. So, both modes were inverted with error floors of 10% for ρ_{TE} and ρ_{TM}, 1.45° for φ_{TM} and φ_{TE}. The model for profile P-2 and pseudosection measured data as well as model responses are shown in Fig. 5B.

Inversion of separate modes, TE and TM, for profile P-3 roughly results in the same model. So, both modes were inverted with error floors of 10% for ρ_{TE} and ρ_{TM}, and 1.45° for φ_{TM} and φ_{TE}. The model for profile P-3, pseudosection measured data and model responses are shown in Fig. 6.

The depth and lithology obtained in all the models agree with those observed in the wells. For all the models, interpretation was not restricted by the skin depth, calculated using the integrated conductance, because it was much greater than the maximum depth of the model, except for the west end of model P-2. The skin depth of this model presents a sharp drop at site 7 (dashed white line in model P-2 Fig. 5B).

All inversions converged to smooth models with small roughness and NRMS close to 1. The variation of NRMS by site is shown with each model. The geometry of the basin bottom is resolved for all the profiles. In profile P-1, the distance between consecutive sites is less than in the other profiles because changes in the depth at which the basement is found were observed to be more pronounced along this profile.

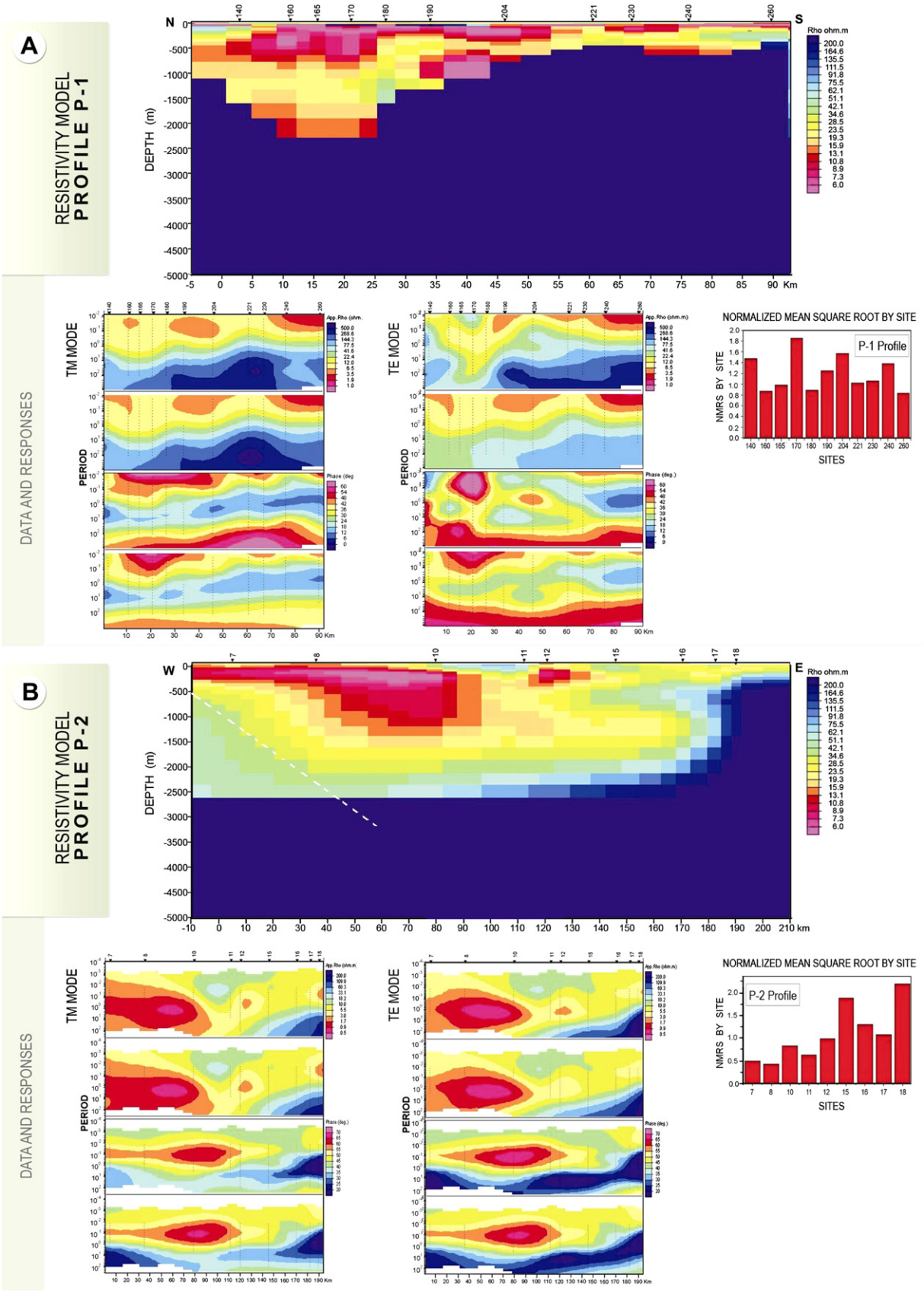

Fig. 5. A) Model for profile P-1, (100 km long, 5 km deep) in the scale 5-200 Ω-m, total NRMS by site and pseudosection data (upper panel) and model predicted response (lower panel). B) Model for profile P-2, (200 km long, 5 km deep) in the scale 5-200 Ω-m, total NRMS by site and pseudosection data (upper panel) and model predicted response (lower panel). Dashed line shows the calculated skin depth at the western end.

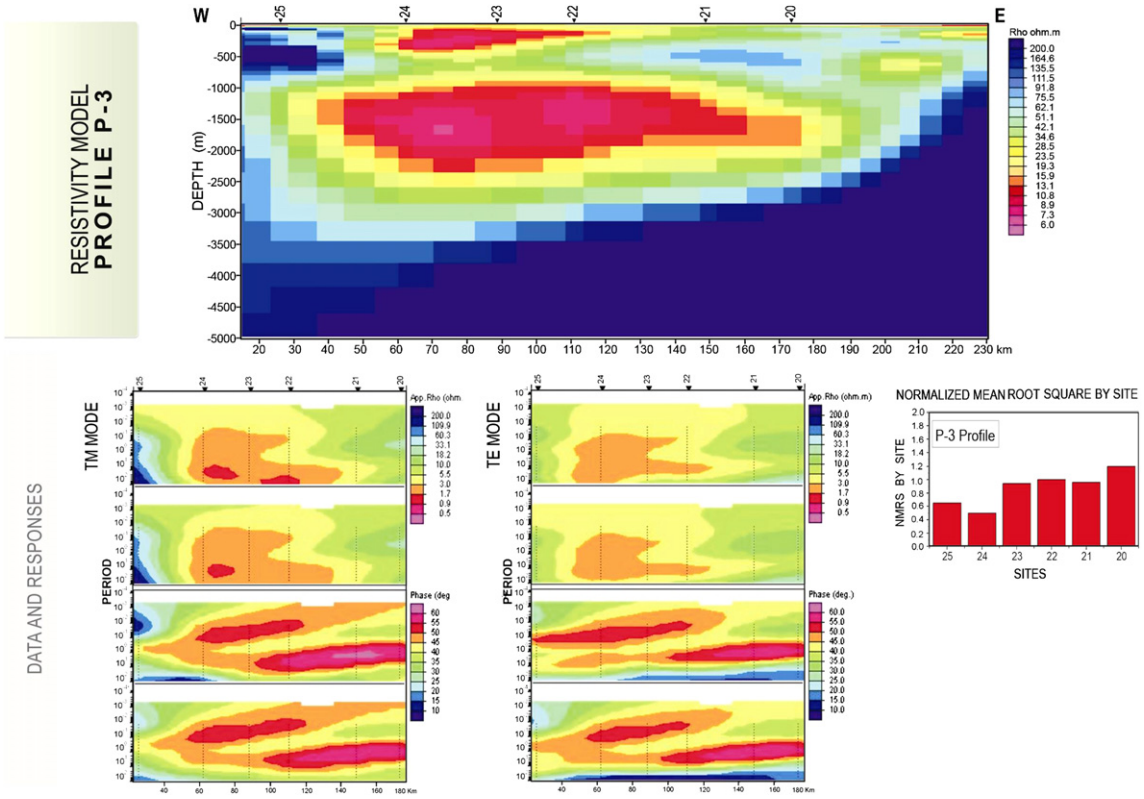

Fig. 6. Model for profile P-3, (200 km long, 5 km deep) in the scale 5-200 Ω-m, total NRMS by site and pseudosection data (upper panel) and model predicted response (lower panel) pseudosection data (upper panel) and model predicted response (lower panel).

The trade-off curves of NRMS versus model roughness have been calculated and the value of parameter τ was set to 3 with regular criteria (e.g. Favetto et al., 2007).

5. Discussion and conclusions

The top of the basement is a hydrogeological controlling structure, relevant to defining overlying formations. The presence of basalts is very important for the confinement of SAG. The capability of the MT method to determine the upper and lower limits of the basalts depends on thickness and resistivity contrasts between contiguous formations. In Entre Rios, basalts have been observed in some wells with several intercalations of sandy intrusions containing extremely salty water (e.g. Villaguay well by Stöckli et al., 2006). In such cases resistivity discrimination is hardly viable.

Our previous magnetotelluric study in this zone was made using long period magnetometers at 31.5°S. That study processed 22 sites to obtain a 2D model showing the geometry of the crystalline basement. The deepest part of the basin is found in the center of profile WE, (Fig. 3, sites 851 to 895), where it reaches a depth of 4000 m. At the eastern end, depth decreases to around 3000 m. Resistivity values within the basin range from 1 to 10 Ωm, which correlates positively with data from Villaguay-1 well.

In MT models, some zones along the profiles do not allow to identify the boundaries between the most important aquifer-related formations.

The presence of saline water in the basalts causes the whole basin to be very conductive. This makes it impossible to determine the thickness and depth of the basalts within the basin.

All the models show high contrast between the sediments and the basement. In model P-1 a very conductive structure can be observed close to the surface and reaching 500 m deep with resistivities lower than 1 Ohm-m. Beyond this, a more resistive zone is well discriminated when the inversion is constrained by a tear at the basin bottom boundary. This area (yellow in the model) could correspond to the basalts. Contours in Fig. 2 show increasing thickness of the basalts from 200 to 500 m (S to N), in the model a thicker part (~900 m) seems to be present where the basement is deeper (up to 2000 m). Thermal water drillings over the P-1 profile, Gualeguaychú 1 and 2, are located near to sites 190 and 204. In these wells a basalt layer was found from 450–473 m to 635–729 m and the basement reached 815–988 m deep (Table 2). These values are consistent with the model. The deepest part of the basin reaches a depth of 2200 m and is located 20–30 km north of Gualeguaychú.

Model P-2 shows a structural high in the eastern end, the basement at around 500 m deep. Everywhere else in this profile, average sediment thickness is around 2500 m. From site 11 to site 17 the basalts are found between 300 m and 1000 m deep. These results are equivalent to the values found in the thermal water drilling over this profile (Villa Elisa, close to site 19, see Table 2). To the west of site 11 the conductive part of the basin reaches greater depths which may indicate that basalts cannot be discriminated by means of their resistivity. Due to limited depth resolution at the west end, it was not possible to determine the basin bottom.

In model P-3, the average depth of the basin is around 2500 m. There is a layer from around 400 to 900 m that could be interpreted as basalt, coincident with the inferred contours in Fig. 2. The layer seems to be less fractured or to have intercalations with low salt content. Beyond that layer there is a very conductive zone from about 1000 to 2000 m associated to the SAG, the inferred top of which is from 1000 to 1100 (Fig. 2). The well over this profile is located in La Paz, exactly at the northwestern end. Model results agree with well data.

Because our MT surveys clearly identify the depth to the basement in the region of the Guaraní aquifer, they are of considerable significance for water resource exploration. In particular, our results can be used to constrain interpretation of more local geoelectrical exploration using controlled-source techniques such as Vertical Electric Sounding. VES is a widely used technique to determine layered model at a given location, the resolution in determining the basement depth when it is greater than 1000 m is very poor, as in this area.

Acknowledgments

We are especially grateful to Dr. Cristina Dapeña for her valuable comments; to Daniel Mársico, for kindly providing us with information on the wells, and to Eduardo Llambías for his help in the fieldwork.

This study was supported by the Argentine Consejo de Investigaciones Cientificas y Tecnicas (CONICET, grant PIP 5448).

References

Arango, C., Marcuello, A., Ledo, J., Queralt, P., 2009. Characterization of the geothermal anomaly in the Llucmajor aquifer system (Majorca, Spain). J. Appl. Geophys. 68 (4), 479–488.

Araújo, L., Franca, A., Potter, P., 1999. Hydrogeology of Mercosul aquifer system in the Paraná and Paraná basins, South America, and comparison with the Navajo-Nugget aquifer system, USA. Hydrogeol. J. 7, 317–336.

Bahr, K., Simpson, F., 2005. Practical Magnetotellurics. Cambridge University Press, ISBN 978-0521817271, 270 pp.

Bernard, T., Nolan, D., Campbell, R., Senterfit, M., 1998. Depth of the base of the Jackson aquifer, based on geophysical exploration, Southern Jackson Hole, Wyoming, USA. Hydrogeol. J. 6 (3), 374–382.

Bibby, H.M., Caldwell, T.G., Brown, C., 2005. Determinable and non-determinable parameters of galvanic distortion in magnetotellurics. Geophys. J. Int. 163 (3), 915–930.

Booker, J., Favetto, A., Pomposiello, M.C., 2004. Low electrical resistivity associated with plunging of the Nazca flat slab beneath Argentina. Nature 429, 399–403.

Caldwell, T.G., Bibby, H.M., Brown, C., 2004. The magnetotelluric phase tensor. Geophys. J. Int. 158, 457–469.

Campos, H., 2000. Mapa hidrogeológico del Acuífero Guaraní. Proceedings of the 1st. Joint World Congress on Groundwater, Fortaleza, Brasil, pp. 15, (in CD format).

Chebli G.A., Mozetic M.E., Rossello E.A. Buhler M., 1999. Cuencas Sedimentarias de la Llanura Chacopampeana. In: Caminos, R. (Ed.), Geología Argentina, SEGEMAR. Anales 29 (20), 627 –644. Buenos Aires.

Egbert, G., Booker, J., 1987. Robust estimation of geomagnetic transfer function estimation. Geophys. J. R. Astron. Soc. 87, 173–194.

Favetto, A., Pomposiello, C., Sainato, C., Dapeña, C., Guida, N., 2005. Estudio geofísico aplicado a la evolución del recurso geotermal en el sudeste de Entre Ríos. Rev. Assoc. Geol. Argent. 60 (1), 197–206.

Favetto, A., Pomposiello, M.C., Booker, J., Rossello, E.A., 2007. Magnetotelluric inversion constrained by seismic data in the Tucumán basin (Andean Foothills, 27°S, NW Argentina). J. Geophys. Res. 112, B09104. doi:10.1029/2006JB004455.

Favetto, A., Pomposiello, M.C., López de Luchi, M., Booker, J., 2008. 2D Magnetotelluric interpretation of the crust electrical resistivity across the Pampean Terrane–Río de la Plata suture, in Central Argentina. Tectonophysics 459, 54–65.

Favetto, A., Pomposiello, M.C., 2009. Modelo Geoeléctrico de la cuenca Chacoparanense en Santa-Fé-Entre Ríos (NE, Argentina) a partir de un estudio magnetotelúrico (submitted to Rev. Asoc. Geol. Argentina).

Gentili, C., Rimoldi, H., 1979. Mesopotamia, 1. Academia Nacional De Ciencias, Segundo Simposio Geología Regional Argentina. Córdoba185–223.

Mársico D.P., 2009. Aportes a la perspectiva geológica e hidrogeológica regional en el sector centro-este de la cuenca chacopampeana, personal communication.

McNeice, G., Jones, A., 2001. Multi-site, multi-frequency tensor decomposition of magnetotelluric data. Geophysics 66, 158–173.

Montaño, X., Tujchneider, O., Auge, M., Fili, M., Paris, M., D'elia, M., Pérez, M., Nagy, M.I., Collazo, P., Decoud, P., 1998. Acuíferos Regionales en América Latina. Sistema Acuífero Guaraní. Capítulo Argentino-Uruguayo. Centro de Publicaciones, Secretaría de Extensión, Universidad Nacional del Litoral, Santa Fé, Argentina, pp. 217.

Montaño, J., Da Rosa Filho, E., Hernández, M., 2004. Características hidrogeológicas del Sistema Acuífero Guaraní (Hydrogeological characteristics of the Guaraní Aquifer System). http://www.alhsud.com/castellano/articulos_listado.asp Cited 01 Abr 2004.

Parker, R., Booker, J., 1996. Optimal one-dimensional inversion and bounding of magnetotelluric apparent resistivity and phase measurements. Phys. Earth Planet. Inter. 98, 269–282.

Ramos, V., Cristallini, E.O., Perez, D., 2002. the Pampean flat-slab of the Central Andes. J. S. Am. Earth Sci., 59–78.

Rodi, W., Mackie, R., 2001. Nonlinear conjugate gradient algorithm for 2-D magnetotelluric inversion. Geophysics 66, 174–178.

Sanford, R., Lange, F., 1960. Basin study approach to oil evaluation of Paraná miogeosyncline, South Brazil. Am. Assoc. Pet. Geol. Bull. 44 (8), 1316–1370.

Silva Busso, A. 1999. Contribución al conocimiento de la geología e hidrogeología del Sistema Acuífero Termal de la Cuenca Chacoparanense Oriental Argentina (Contribution to the geological and hydrogeological knowledge of the Thermal Aquifer System in the East Chacoparanense Basin). Thesis, University of Buenos Aires, Argentina. [in Spanish].

Stöckli, F., Dapeña, C., Stöckli, M., 2006. El Pozo Termal Villaguay-1, Provincia De Entre Ríos, Argentina. Viii Congreso Latinoamericano De Hidrología Subterránea. Alhsud Volumen Cd T-02, Asunción, Paraguay, 14 p.

Tujchneider, O., Pérez, M., Paris, M. D'Elia M., 2006. The Guaraní Aquifer System: State of the art in Argentina. International Simp. Aquifer System Management, 2006, Dijon, France.

Volpia, G., Manzella, A., Fiordelisib, A., 2003. Investigation of geothermal structures by Magnetotellurics (MT): an example from the Mt. Amiata area, Italy, 2003. Geothermics 32, 131–145.

White, I.C., 1908. Relatorio sobre as "Coal measures" e rochas asociadas do sul do Brasil. In: Relatório Final da Comissaõ de Estudos das Minas de Carvaõ de Pedra do Brasil, 1. Impresa Nacional, Río de Janeiro. 2–300.